Peer-reviewed version available at *Energies* **2020**, *13*, 1119; doi:10.3390/en13051119

Article

Petrographic characteristics of sandstones as a basis to evaluate their suitability in construction and energy storage applications. A case study from Klepa Nafpaktias (Central Western Greece).

Petros Petrounias [1,*], Panagiota P. Giannakopoulou [1], Aikaterini Rogkala [1], Maria Kalpogiannaki[1], Petros Koutsovitis[1], Maria-Elli Damoulianou[1], Nikolaos Koukouzas[2]

[1] Section of Earth Materials, Department of Geology, University of Patras, 26504, Patras, Greece; peny_giannakopoulou@windowslive.com (P.P.G.); krogkala@upatras.gr (A.R.); maria.kalpogiannaki@gmail.com (M.K); pkoutsovitis@upatras.gr (P.K); marilliedam@gmail.com (M.E.D);

[2] Chemical Process & Energy Resources Institute, Centre for Research & Technology Hellas (CERTH), Greece; koukouzas@certh.gr (N.K)

* Correspondence: Geo.plan@outlook.com

Abstract: This paper examines the influence of the petrographic characteristics of sandstones from Klepa Nafpaktias (Greece) on their suitability in construction (concrete) and energy storage applications. For this scope, ten sandstones were collected in order to study their petrographic characteristics using petrographic microscope and a GIS software as well as their basic physical, mechanical and physicochemical properties. Concrete specimens (C25/30) were produced with constant volume proportions, workability, mixing and curing conditions using different sizes of each aggregate type. Aggregates were mixed both in dry and water saturated states in concrete. Three different types of sandstone aggregates were examined and classified in three district groups according to their physicomechanical properties, petrographic characteristics and surface texture. The classification in groups after the concrete compressive strength test (UCS) verified the initial classification in the same three groups relative to their grain size from coarse to fine grained. As the grain size decreases their physicomechanical and physicochemical properties are getting better resulting in higher concrete strength values (25 to 32 MPa). Furthermore, the proposed ratio C/A (crystals/ mm^2) seems to influence the aggregate properties which constitute critical factors for the final concrete strength, presenting the more fine grained sandstones as the most suitable for concrete aggregates. Concerning the use of Klepa Nafpaktias sandstones as potential energy reservoirs, the studied sandstones have the appropriate physicochemical properties for the implementation of a financially feasible CO_2 capture and storage scenario.

Keywords: petrographic characteristics; sandstones; physicomechanical properties; concrete petrography; CO_2 storage

1. Introduction

Applied petrography constitutes an essential tool for the assessment of natural rocks or recycling materials for different useful applications such as concrete and energy storage applications. Petrography, generally, using a combination of methods such as microscopic observations (polarizing and scanning electron microscope) and chemical analysis examines the nature of each given rock/material showing the main relationships of texture, structure, composition and alteration degree [1-9]. Through these relationships, petrography may explain the physicomechanical and physicochemical properties of materials/rocks as well as the relationships among them. It is well-known that the already above mentioned properties are the critical ones which define the particular use of each given material/rock either construction or environmental applications.

Peer-reviewed version available at Energies 2020, 13, 1119; doi:10.3390/en13051119

Concrete is one of the most important and useful composite material, which is made from a mixture of cement, aggregates, water and sometimes admixtures in required proportions [10-13]. The main component is a mixture of cement and water which binds the aggregate particles in a strong mass. Aggregates are the major constituents of concrete as occupy between 70% and 80% of the concrete volume [10]. However, the quality of aggregate, including its long-term durability and resistance to cracking, influence the properties of both fresh and hardened concrete [11-13]. The inhomogeneous structure of concrete can be described as a three-phase system consisting of hardened cement paste, aggregate and the interface between aggregate particles and cement paste [14]. Natural coarse aggregates are various crushed rocks extracted from pits and quarries of different geological sources [15]. The physico-mechanical properties of aggregates are the most significant parameters in any application and in their classification for various engineering purposes. Physicomechanical properties depend on the petrographic characteristics which plays a critical role on its strength and therefore on concrete strength. The most common types of rocks used in concrete production are classified into igneous, sedimentary and metamorphic rocks. Aggregates can be expected to have an important influence on the concrete's properties [16]. Such rocks are mainly limestone, granite, sandstone, quartzite, dolomite, marble, dacite etc. Each of these rock types is more or less suitable for uses as concrete aggregates, based on their petrographic characteristics and therefore on physicomechanical properties which contribute to reinforcing the strength of the concrete.

Sandstone is a widespread aggregate resource used in concrete construction around world. The geological properties of this sedimentary rock are fairly diverse and aggregates such as quartzite, subarcose and greywacke can produce a range of hardened concrete properties. Therefore, it is important that sandstone aggregates can be easily characterized to obtain predictable aggregate and concrete properties [17]. Sandstone used as aggregate of different sizes in concrete would have a varying effect on its corresponding strength and further it is important to grade these aggregates when used in concrete. Moreover, sandstone is affected by the influence of moisture which is known that decreases the mechanical properties of brittle construction materials. However, these sedimentary rocks are tend to have lesser compressive strength than conventional aggregates and have distributed plots on mechanical properties and are very sensitive to time-dependent mechanical deterioration. Sandstones perform well in dry condition but in a wet condition it is poor specifically for less cemented sandstone types [18, 19]. The quartz content in concrete prepared by sandstone aggregates determines the concrete application [20]. Yilmaz & Tugrul [21] reported that for the same quality of cement and quantity of cement, different types of sandstone aggregates with different mineralogical composition, cement type, texture and therefore physical and mechanical properties may result in different concrete strengths.

Many researchers have investigated the correlations between the percentages of specific mineralogical compositions of aggregates and the final compressive concrete strength. Petrounias et al. [22, 23] when investigating igneous rocks from Greece concluded that the secondary products of serpentinites and andesites largely influence their mechanical properties, which definitely have an adverse effect on their performance as concrete aggregates. On the other hand, Yılmaz & Tugrul [21] evaluate the composition, physical and mechanical properties of different sandstone aggregates on the strength of concrete and they have concluded that for the same quality and quantity of cement, different types of sandstone aggregates from Turkey with different mineralogical composition, texture and therefore physical and mechanical properties result in different concrete strengths.

During the last decades, only a few attempts to combine the database and visualization facilities of Geographic Information System (GIS) software and petrographic features of rocks have been carried out. In these studies, polarizing microscope images have been used in order to identify and visualize rock textures on microscopic scale. Li et al. [24] use GIS software for the segmentation and analysis of grain boundaries, presenting a procedure tested on a few samples. Barraud [25] applies GIS software to refine and analyze the vectorized texture obtained after segmenting transmitted light microscopy images with third party software. Fernandez et al. [26] use GIS software to compute shape-fabric parameters and strain factors from grain boundary maps. Tarquini [27] has presented a methodology combining GIS and petrographic characteristics of various rocks which

Peer-reviewed version available at Energies 2020, 13, 1119; doi:10.3390/en13051119

constitutes a Microscopic Information System (MIS) and can substitute for a standard petrographic microscope in carrying out preliminary thin section analysis.

Economic growth and a rising global population means that the worldwide demand of energy will be rising with very fast pace. This increases concerns that the extensive use of fossil-fuels should be mitigated, allowing space for further development of renewable energy sources. The problem which arises with the use of the latter is that most of these sources are intermittent and therefore energy storage applications are necessary to make them available around-the-clock for uninterrupted power supply [28]. Suitable subsurface geological formations can serve as energy storage reservoirs depending on the storage purpose and the type of energy source. Energy storage systems include that of thermal energy, CO_2, compressed air, hydrogen storage, natural gas and underground pumping of water.

Rocks consisting geological formations must fulfill certain criteria to be considered as a candidate reservoir for potential thermal-energy storage (TES), compressed air energy storage (CAES) and carbon capture and storage (CCS) applications. These criteria have been noted by researchers [e.g. 28-30] stating that rocks should display high values of the thermal conductivity, specific heat capacity, and density to enable high storage efficiency. Low porosity values correlate positively with high values of bulk density and uniaxial compressive strength, which are necessary to ensure not only the optimum energy storage criteria but to avoid fracture development and disintegration [28]. Research conducted by Allen et al. [31] and Tiskatine et al. [32] suggest that formations consisting of sandstones may serve as proper energy storage reservoirs, provided that they meet compositional (e.g. calcium-or silica-rich), textural and structural and also not having been significantly affected secondary alteration processes.

Aim of this study is to highlight the effect of petrographic characteristics of sandstones from Klepa Nafpaktias (central western Greece) as a decisive factor in the final strength of the produced concrete specimens by sandstones aggregates and also to examine their potential use as geological reservoir for carbon capture and storage (CCS) applications.

2. Geological setting

The study area is Klepa Nafpaktias which geographically belongs to the regional unit of Aitolia and Akarnania and geologically to the Pindos Geotectonic Zone, which comprises an intricate thrust belt with allochthonous Mesozoic and Tertiary deep-water tectono-stratigraphic units [33], which are developing along the central Western Greece (Figure 1) and extend into Albania and former Yugoslavia to the north [34], and Crete, Rhodes [35], and Turkey [36, 37], towards the south and southeast. The Pindos Zone sedimentary sequence was deposited in an elongated ocean basin that was formed in mid-Triassic, along the north-eastern passive margin of Apulia platform [38], between the extensive Gavrovo-Tripolis platform [33, 39] that emerged periodically, and now lies westwards of Pindos, and the Pelagonian continental block in the east [40-43]. The progressive closure of the Pindos oceanic basin initiated during the end of Maastrichtian, as recorded by the gradual alteration, from predominantly carbonates intercalating with radiolaria to siliciclastic/ turbiditic lithofacies (Paleocene flysch deposition) derived from the north and east sectors [33, 39, 44]. The complete closure of the Pindos Ocean during the Eocene led to the detachment of the deep-sea sedimentary cover from the oceanic basement as an accretionary prism, which was later emplaced westwards onto the carbonate platform, forming a series of thin-skinned thrust sheets [38, 42].

Peer-reviewed version available at Energies 2020, 13, 1119; doi:10.3390/en13051119

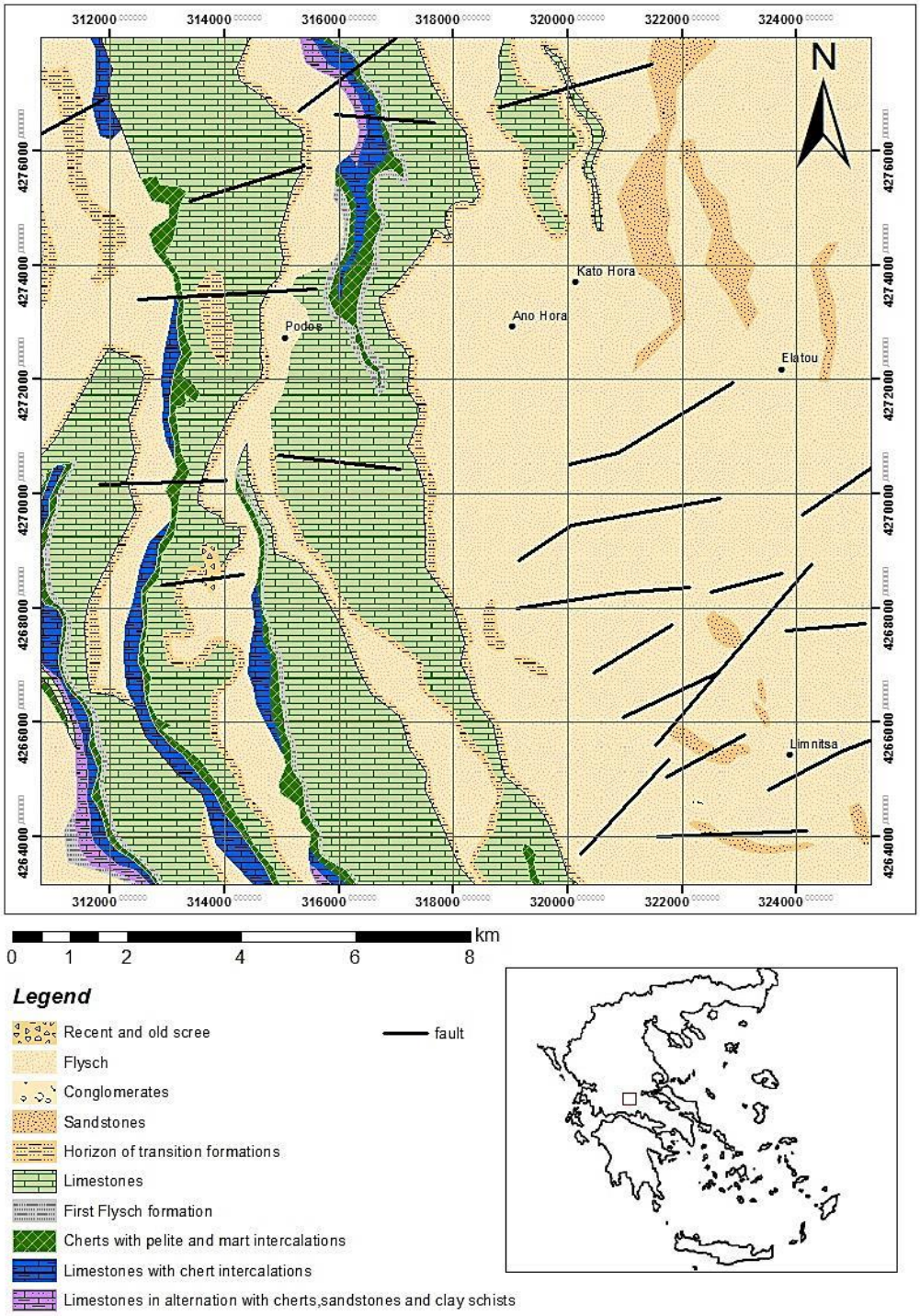

Figure 1. Geological map of the Klepa Nafpaktias [49] (Central Western Greece) region (modified after fieldwork mapping by using ArcMap 10.1).

The sedimentary alternating strata of Pindos Zone consist of deep-water carbonate, siliciclastic and siliceous rocks of Late Triassic to Eocene age [38, 39, 42], mainly including the following units (Figure 1) the Pindos Ophiolites (Jurassic), 2) the shallow water Orliakas limestones (Late Cretaceous), 3) the Avdella Mélange (Late Triassic—Late Jurassic), 4) the Dio Dendra Group deep-water sediments (Late Jurassic—Late Cretaceous) and 5) the Pindos flysch (Late Cretaceous—Tertiary) according to Jones & Robertson [46]. More extensively, the Pindos flysch consists of thin- to thick-bedded sandstones and mudstones in alteration with marly-oolitic

Peer-reviewed version available at Energies 2020, 13, 1119; doi:10.3390/en13051119

limestones and cherts (reference). According to Konstantopoulos and Zelilidis [45], the sandstones of the Pindos Flysch were probably deposited in an active continental margin, or a continental island arc provenance, supplied by predominantly basic/ultra-basic and less felsic material. Furthermore, Faupl et al. [47] conducted a heavy mineral examination, suggesting that the clastic material of the Pindos flysch has an eastwards origin, while a petrographic and geochemical study by Vakalas et al. [48] on sandstone samples from Epirus and Akarnania regions suggests a granitic source and a supply from the Pelagonian Zone correspondingly. Detrital modes of sandstone suites reveal the lithological composition of source terranes and the tectonostratigraphic level reached by erosion in space and time.

3. Materials and Methods

3.1 Materials

Ten samples from different type of sandstones (coarse grained and fine grained) were collected from the studied area. These samples were tested for their petrographic characteristics, physicomechanical and physicochemical properties in order to be classified for their suitability as concrete aggregates. The type of cement used in this study was Normal Portland cement (CEM II 32.5N), which conformed to EN 197-1 [50] was used with the aggregates for the production of concrete. Potable tap water with pH=7, free of impurities such as salt, silt, clay and organic matter, was used for mixing and curing the concrete. In order to keep a consistent composition for all the concrete specimens, we adopted the principle of maintaining the same volume of aggregate per m^3 of the mixture. The proportions of the concrete mixtures, by mass, were 1/6/0.63 cement, aggregate and water ratio. The same collected sandstones were also investigated for their potential use as reservoir for thermal-energy storage (TES) and compressed air energy storage (CAES) applications.

3.2 Methods

3.2.1 Rock material tests

The mineralogical and textural characteristics of the collected sandstone samples were firstly examined in polished thin sections with a polarizing microscope according to EN-932-3 [51] standard for petrographic description of aggregates. The thin sections were examined under a polarizing microscope (Leitz Ortholux II POL-BK Ltd., Midland, ON, Canada) for mean grain size and grain shape. The petrographic characteristics of the tested sandstones were studied as well as the quantification of their mineralogical composition was calculated using the ArcMap 10.1 software, in which 6 representative thin sections of the studied groups (two per sample) were investigated.

The surface texture of aggregate samples was studied by using Secondary Electron Images (SEI) according to BS 812 Part 1[52] which outlines six qualitative categories, e.g. glassy, smooth, granular, rough, crystalline, honeycomb and porous.

Then the studied sandstone samples were crushed into smaller pieces by hammer. Aggregate fractions were prepared from the smaller pieces using a laboratory jaw crusher. Laboratory core drill and saw machines were used to prepare cylindrical specimens which their diameters range between 50 and 54 mm and the ratio of length to diameter was between 2.2 and 2.5 mm.

The physicomechanical properties which were studied for the tested samples were the total porosity (n_t) which was calculated using specimens of rocks according to the ISRM 1981 standard [53], the magnesium sulfate (MgSO4) test according to the EN 1367-2 standard [54] and the water absorption (w_a) which constitutes major property in evaluating the durability of rocks as aggregates according to EN 1097-6 [55]. The resistance to fragmentation of the crushed sandstone aggregates was examined using the Los Angeles (LA) abrasion machine according to the ASTM C-131 [56] and the uniaxial compressive strength (UCS) was tested on core cylindrical samples, according to the ASTM D 2938-95 (2002) specification [57].

Peer-reviewed version available at Energies 2020, 13, 1119; doi:10.3390/en13051119

3.2.2 Concrete tests

Twenty normal concrete cube specimens (150×150 mm) were made from the ten investigated sandstone aggregates (Table 1) according to ACI-211.1-91 [58]. All of the parameters remained constant in all the concrete specimens. The aggregates were crushed and sieved through standard sieves and separated into the size classes of 2.00-4.75, 4.45-9.5 and 9.5-19.1 mm. After 24h, the samples were removed from the mold and were cured in water for 28 days. Curing temperature was 20±3 ^{o}C. These specimens were tested in a compression testing machine at an increasing rate of load of 140 kg/cm^2 per minute. The compressive strength of concrete was calculated by the division of the value of the load at the moment of failure over the area of specimen. The compression test was elaborated according to BS EN 12390-3:2009 [59].

After the compressive strength test, the textural characteristics of concrete specimens were examined. Polished thin sections were studied in a polarizing microscope according to ASTM C856 – 17 [60]. A 3D depiction of the petrographic characteristics of the concrete as well as of the studied sandstone aggregates was carried out by the 3D Builder software using thin sections.

4. Results

4.1 Test results of aggregates

4.1. 1. Petrographic features of aggregates using petrographic microscope

The studied sandstones derived from Klepa area have been divided according to the petrographic analysis into three district groups. These groups are based on the grain size of the collected sandstones and they were characterized as coarse to fine grained ones.

Group I: Coarse- grained sandstones (KL.5, KL.9)

These sandstones comprise sub-angular to angular grains (Figure 2a,b). They are generally moderate to poor sorted. The mineralogical composition mainly includes quartz, K-feldspars, plagioclase, calcite, mica and in minor amounts muscovite, chlorite and biotite as well as lithic fragments (Table 1). These sandstones present mainly siliceous cement. Quartz is mostly present as undulose monocrystalline and less as polycrystalline grains. The monocrystalline quartz grains range from sub-angular to angular, whereas the polycrystallines vary from sub-angular to sub-round. The grain contacts are straight to suture. K-feldspars grains vary in size, from small to large with euhedral to subhedral shape, whereas plagioclase is observed in smaller grains. In general, the fragments are sub-rounded and sub-angular to angular and they are mainly comprised of clasts of quartz, feldspars as well as by rock-fragments of basalt and gabbro. Traces of carbonate fossils are also observed in several samples (e.g. KL.5).

Group II: Medium-grained sandstones (KL.1, KL.2, KL.3, KL.6)

The medium-grained sandstones can be classified as quartz sandstones. They are moderately sorted and their grains are sub-angular to sub-round. The main mineralogical composition includes quartz which forms monocrystalline and polycrystalline grains, K-feldspars, calcite and muscovite (Figure 2c). Polycrystalline quartz shows interlocking texture. Feldspars (mainly microcline) are presented in lesser amounts, including the weathered varieties (Table 1). Cement is mainly siliceous and locally calcareous.

Peer-reviewed version available at *Energies* **2020**, *13*, 1119; doi:10.3390/en13051119

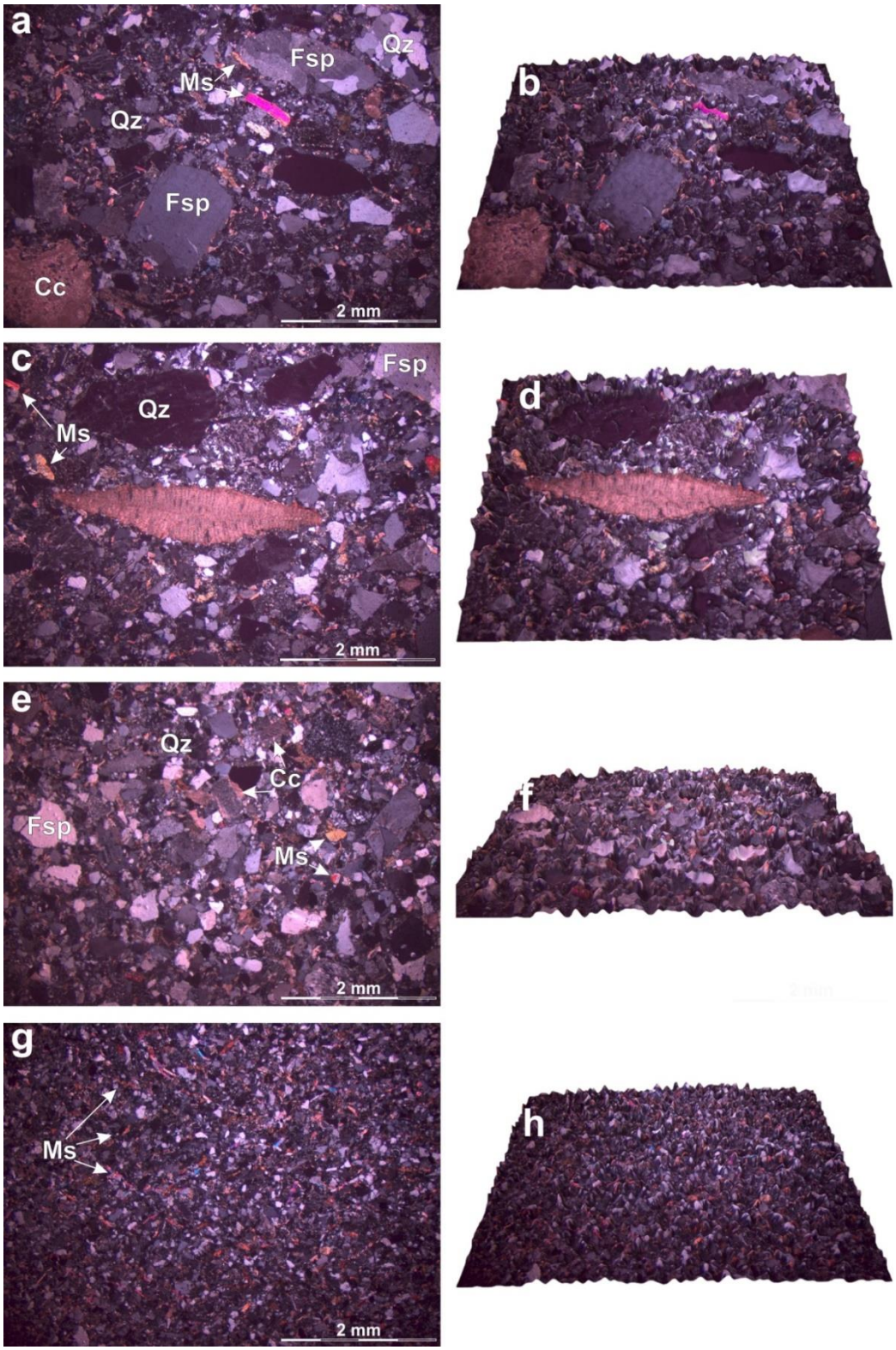

Figure 2. Photomicrograph of textural characteristics of sandstone aggregates (Nicols+) and 3D depiction of the studied sandstones respectively: (**a**) clastic texture presented in a coarse grained quartz sandstone with quartz (qz), K-feldspars (K-Fs), plagioclase (Plg), muscovite (Ms) and calcite (Cc) (sample KL.5); (**b**) 3D depiction of coarse grained sandstone (sample KL.5); (**c**) clastic texture presented in a coarse grained sandstone containing large particles of carbonate fossils (sample KL.9); (**d**) 3D depiction of coarse grained sandstone (sample KL.9); (**e**) clastic texture presented in a medium grained quartz sandstone with quartz (qz), K-feldspars (K-Fs) and calcite (Cc) (sample KL.3); (**f**) 3D depiction of coarse grained sandstone (sample KL.3); (**g**) clastic texture presented in a fine grained

Peer-reviewed version available at Energies 2020, 13, 1119; doi:10.3390/en13051119

quartz sandstone with muscovite (Ms) (sampleKL.7); (**h**) 3D depiction of fine grained sandstone (sample KL.7).

Group III: Fine-grained sandstones (KL.4, KL.7, KL.8, KL.10)

In the fine-grained quartz sandstones, framework grains are mainly sub-angular to sub-round. They are characterized as well sorted quartz sandstones. The modal composition mostly comprises of quartz, K-feldspars, calcite and mica (mainly muscovite) which is presented in bigger amounts in contrast to the other two groups. Cementing material is mainly siliceous (Table 1).

4.1.2. Petrographic features of aggregates using GIS method

In this paper, GIS method was used as a new approach for petrographic analysis of the investigated sandstones. For this reason, six thin sections, representative of the investigated sandstones (two sections for each group) were used in order to be analyzed via GIS method. More specifically, a part of the same size and in the same site of the thin section has been chosen to be digitized via ArcMap 10.1 software. Each digitized polygon corresponds to a different grain of the sandstone. The result of that process is the creation of a map which shows the modal composition of the tested rocks as well as their textural characteristics such as the grain size (Figure 3). In a next stage, the semi-quantification of the mineralogical composition of the studied sandstones was carried out, showing that Group III presents higher content of quartz than the other two groups, Group I displays intense higher content of feldspars in contrast to Group II and III (Table 1), while Group II is presented as more enriched in calcite (Table 1). Furthermore, Group III displays significant high content of muscovite. Concerning the containing cement, Group III presents higher content of silica cement in contrary to the other two groups (Table 1). After the petrographic analysis via the GIS proposed method, the ratio C/A was calculated (Table 1). C/A (crystals/mm^2) is the ratio of the sum of the measured crystals to the measured area (mm^2). As can be seen in Table 1, Group I, which contains the coarser grains, presents an average of C/A 11.60 in contrast to samples of Group III which presents values of C/A from 55.70 to 56.50 and this group consists of the smallest size grains.

Table 1. Quantification of the Modal composition of the representative investigated groups of sandstones

		Modal composition						Ratio
	Samples	Quartz	K-Feldspars	Plagioclase	Calcite	Muscovite	Total cement	C/A
Group I	K.L5	24.96	29.20	0.53	1.43	1.60	42.28	11.61
	K.L9	26.00	28.34	0.51	1.43	1.58	42.14	11.59
Group II	K.L1	25.56	16.82	0.50	8.40	1.37	47.35	21.40
	K.L3	25.52	16.81	0.65	8.05	1.33	47.64	20.80
Group III	K.L7	29.50	6.64	0.20	2.46	4.12	57.08	56.50
	K.L10	29.10	6.62	0.26	2.44	1.41	57.44	55.70

Peer-reviewed version available at Energies 2020, 13, 1119; doi:10.3390/en13051119

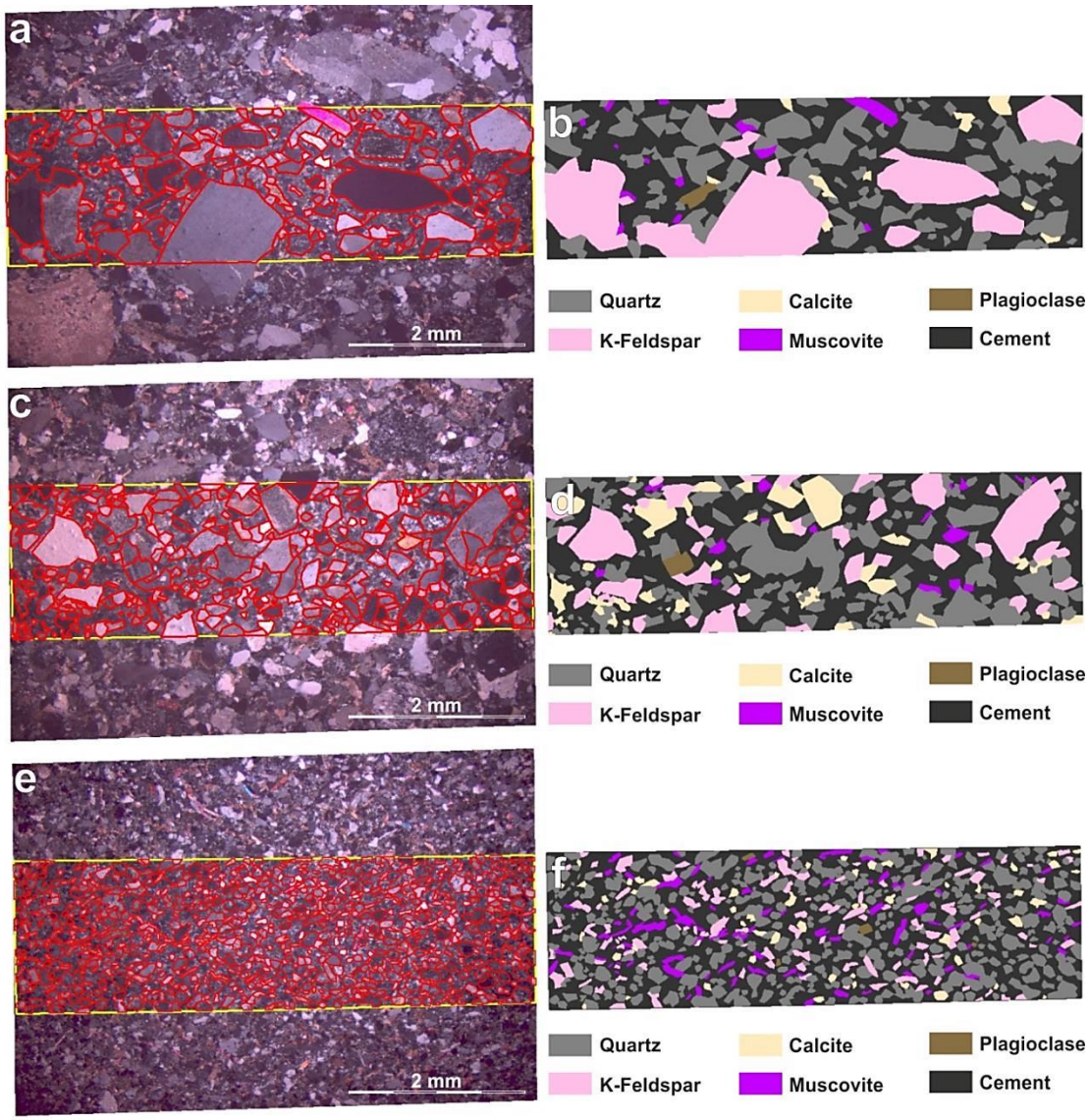

Figure 3. Representative images from the studied groups derived from the ArcMap 10.1 software showing: (**a**) the part of the thin section of the coarse grained sandstone (KL. 5) which has been analyzed; (**b**) the output after the digitalization of the investigated part of each thin section where each mineral phase has been attributed by different colors (KL.5); (**c**) the part of the thin section of the medium grained sandstone (KL. 3) which has been analyzed; (**d**) the output after the digitalization of the investigated part of each thin section where each mineral phase has been attributed by different colors (KL.3); (**e**)the part of the thin section of the fine grained sandstone (KL. 7) which has been analyzed; (**f**) the output after the digitalization of the investigated part of each thin section where each mineral phase has been attributed by different colors (KL.7).

4.1.3. Surface texture of aggregates

The microroughness of the aggregate particles was used to categorize the quartz sandstones in groups consistent with the above mentioned Groups I to III. Particles of Group I show smooth surfaces, due to the abundance of the coarse size grains of quartz, feldspars and carbonate fossils in the poor sorted sandstone (Figure 4). Samples of Group II were medium-grained rocks and were characterized by a rough surface texture (Figure 4). The surface of Group III samples can be characterized as rougher in contrast to the other two groups due to the existence of higher content of evenly distributed mica and quartz expressing topographic low areas combined with feldspars which express lower topographic areas (Figure 4).

Peer-reviewed version available at *Energies* **2020**, *13*, 1119; doi:10.3390/en13051119

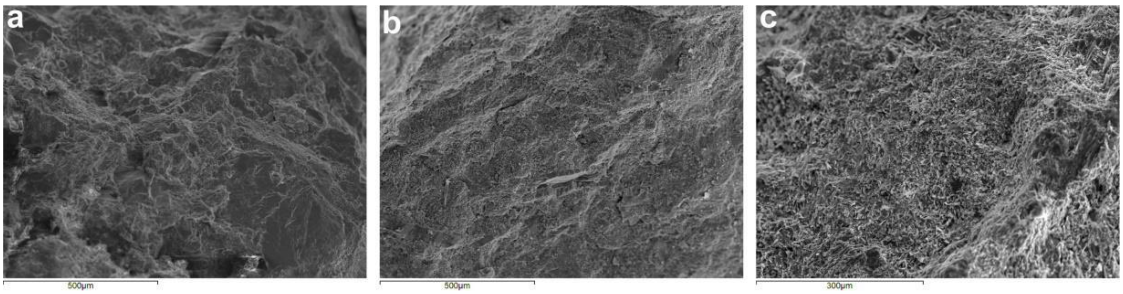

Figure 4. Secondary electron images (SEI) showing the surface texture of representative sandstone samples observed to their mineralogical and textural features: (**a**) coarse grained (KL.5); (**b**) medium grained (KL.2); (**c**) fine grained sandstone (KL.8).

4.1.4. Physico-mechanical properties of aggregates

The results of the physicomechanical properties enabled us to determine three discrete groups (Table 2). Mechanical and physical values of the tested rocks display a wide variation even within the same sedimentary lithology. Three groups of sandstone aggregates were determined in terms of their physico-mechanical properties (Table 2). Group I includes coarse grained sandstones, which displayed the worst values of mechanical properties among all groups (Table 2). Among the studied aggregates of Group I, sample KL.5, which contained lower amount of quartz, gave a lowest value of total porosity (n_t) and resistance in abrasion. Group II was composed of medium grained sandstones (Table 2) showed a wide variance of their physico-mechanical properties due to the variability of their mineralogical features. Group III included fine grained sandstones, which displayed high physicomechanical parameters among all the determined groups. The fine-grained sandstones, such as KL.4 and KL.8, presented better mechanical characteristics against to the coarse-grained sandstones such as KL.5 and KL.9.

Peer-reviewed version available at Energies 2020, 13, 1119; doi:10.3390/en13051119

1 Table 2: The results of the physicomechanical properties of the tested sandstones

Samples	Lithotype	Particle size	Los Angeles (LA %)	Uniaxial compressive strength of rocks (UCS MPa)	n_t (%)	W_a (%)	S (%)
KL.1	Sandstone	Medium grained *(Group II)*	20.0	115.0	4.50	2.10	20.00
KL.2	Sandstone	Medium grained *(Group II)*	21.0	105.0	4.80	1.80	18.00
KL.3	Sandstone	Medium grained *(Group II)*	22.0	89.0	5.30	2.21	19.00
KL.4	Sandstone	Fine grained *(Group III)*	16.0	112.0	3.50	1.55	13.00
KL.5	Sandstone	Coarse grained *(Group I)*	29.0	77.0	9.50	3.30	48.00
KL.6	Sandstone	Medium grained *(Group II)*	19.0	105.0	3.70	2.18	17.00
KL.7	Sandstone	Fine grained *(Group III)*	13.0	115.0	2.30	0.90	15.00
KL.8	Sandstone	Fine grained *(Group III)*	15.0	113.0	2.90	1.50	12.00
KL.9	Sandstone	Coarse grained *(Group I)*	33.0	75.0	19.50	2.80	38.00
KL.10	Sandstone	Fine grained *(Group III)*	15.0	112.0	3.10	1.60	20.00

Peer-reviewed version available at Energies 2020, 13, 1119; doi:10.3390/en13051119

4.2 Test results of concrete

4.2.1 Compressive strength of concrete

The results from the compressive strength test of concrete specimens are listed in Table 3. The concrete strength ranged from 24 to 32 MPa after 28 days of curing. The concrete strength results are in relevant accordance with the strength of their aggregates. The lowest compressive strength values of the concrete specimens were obtained from the samples made with aggregates from Group I (Table 2, 3). More specifically, the coarse grained sandstone which contains carbonate fossils of big size displays the worst strength value (24 MPa), value which is below the permitted limit for the concrete class C25/30. The concrete specimens, made by medium grained aggregates from Group II, showed variance on strength values (26 to 31 MPa), while those made with the finer grained aggregates from Group III presented the highest compressive strength values (30 to 32 MPa).

Table 3. Uniaxial compressive strength test results of the concrete specimens

Samples	Lithotype	Particle size	Uniaxial compressive strength of concrete specimens (UCS_{con} (MPa))
KL.1	Sandstone	Medium grained *(Group II)*	31.0
KL.2	Sandstone	Medium grained *(Group II)*	28.0
KL.3	Sandstone	Medium grained *(Group II)*	26.0
KL.4	Sandstone	Fine grained *(Group III)*	30.0
KL.5	Sandstone	Coarse grained *(Group I)*	25.0
KL.6	Sandstone	Medium grained *(Group II)*	27.0
KL.7	Sandstone	Fine grained *(Group III)*	32.0
KL.8	Sandstone	Fine grained *(Group III)*	32.0
KL.9	Sandstone	Coarse grained *(Group I)*	24.0
KL.10	Sandstone	Fine grained *(Group III)*	31.0

4.2.2 Petrographic features of the concretes

Careful microscopic observation of the thin sections of the concrete specimens which were studied by using polarizing microscope as well as through the 3D depiction of the same thin sections showed, in general, satisfied cohesion between the cement paste and the aggregate particles among all the concrete specimens produced by the coarse grained, the medium grained as well as the fine grained sandstones (Figure 5). The existence of intense content of silica cement may enhance the bonding between the sandstone aggregates and the cement paste. Even neither in concrete specimens produced by aggregates of Group I nor in those produced by aggregates of Group II and III, loss of material can be observed nor extensive interaction zones.

Peer-reviewed version available at Energies 2020, 13, 1119; doi:10.3390/en13051119

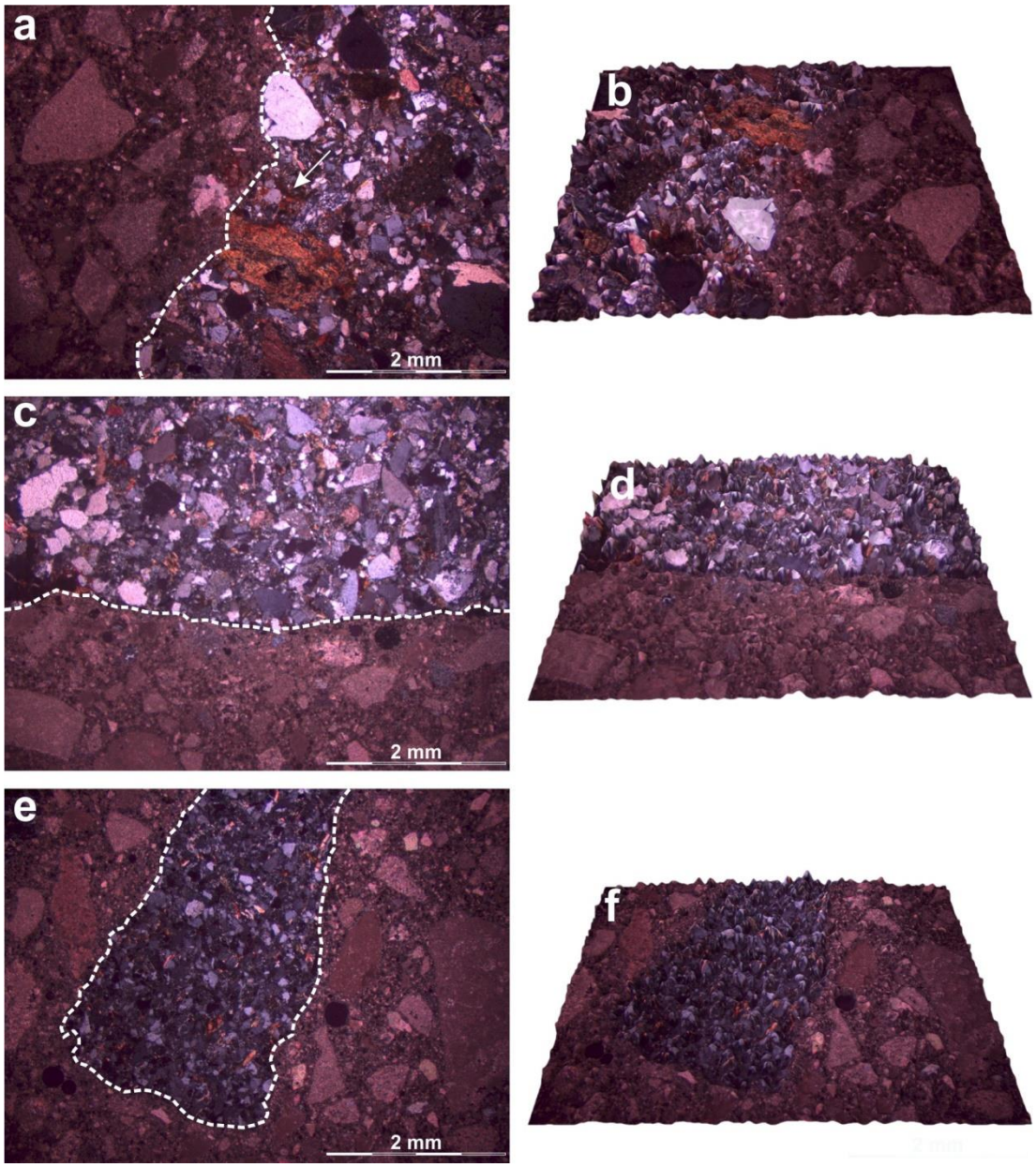

Figure 5. Photomicrographs of representative tested concrete specimens produced by: (**a**) coarse grained sandstone aggregate (KL.5); (**c**) medium grained sandstone aggregate (KL.3); (**e**) fine grained sandstone aggregate (KL.7) and 3D depiction of representative tested concrete specimens produced by: (**b**) coarse grained sandstone aggregate (KL.5); (**d**) medium grained sandstone aggregate (KL.3); (**f**) fine grained sandstone aggregate (KL.7).

5. Discussion

5.1. The impact of petrographic characteristics on the sandstone aggregate properties and on the quality of concrete

Petrographic characteristics such as mineralogical composition, texture, particle size, alteration and weathering degree of rocks which are used as aggregate materials, constitutes the main factors influencing their properties which are critical for their suitability in various construction and industrial applications [61]. A number of researchers have studied the relationships between the physical and the mechanical properties of the aggregate rocks [62-64] giving clear interpretations of these relationships which are based on the type of the contained minerals and on their size. Petrounias et al. [65] have proved that the type of the secondary phyllosilicate minerals contained in mafic, ultramafic and intermediate and acidic volcanic rocks is the critical factor which predominately determines the physico mechanical properties of the studied rocks. Additionally,

Peer-reviewed version available at Energies 2020, 13, 1119; doi:10.3390/en13051119

Tugrul & Zarif [66] have reported that the mean grain size is presented as a primary factor influencing the mechanical behaviour of granites which are used as concrete aggregates. More specifically, they have proved that as the mean grain size decreases, the strength of the rock increases respectively. The most common statistical method used for the determination of the relationships between the various engineering parameters of rocks is the regression analysis [66-68]. In this paper, where sandstones from Klepa Nafpaktias were studied, strong relationships between the physical and mechanical parameters as well as among mechanical, physical and physicochemical ones were observed using regression analysis. These correlations as they presented in Figure 6 are mainly dependent on the grain size and lesser on the mineralogical composition and on the amount of the cement. The diagrams of Figure 6 indicates that as the grain size of the investigated sandstone increases, the values of their physical properties increase while the values of their mechanical properties decrease respectively. For example from the diagram of Figure 6a we can observe that Group I, as it is classified after petrographic analysis through the petrographic microscope and verified after the new proposed petrographic analysis via GIS method and is characterized as the more coarse grained group, presents ratio C/A 11.60 on average and higher values of porosity (n_t) (Table 2) and lower resistance in abrasion and attrition (LA). Likewise in the diagram of Figure 6b Group I presented as more capable to absorb water (w_a) and with lower values of uniaxial compressive strength (UCS). Diagrams of Figure 6a and 6b show the interaction between the physical and mechanical properties which are directly depended on the grain size of the similar mineralogical composition tested sandstones. The lower value of the mechanical strength of the coarse grained sandstones may be a result of the low, and maybe because of the microtopography, internal attrition between the grains combined with the small percentage of cement, which leads to small angles of attrition relative to the density.

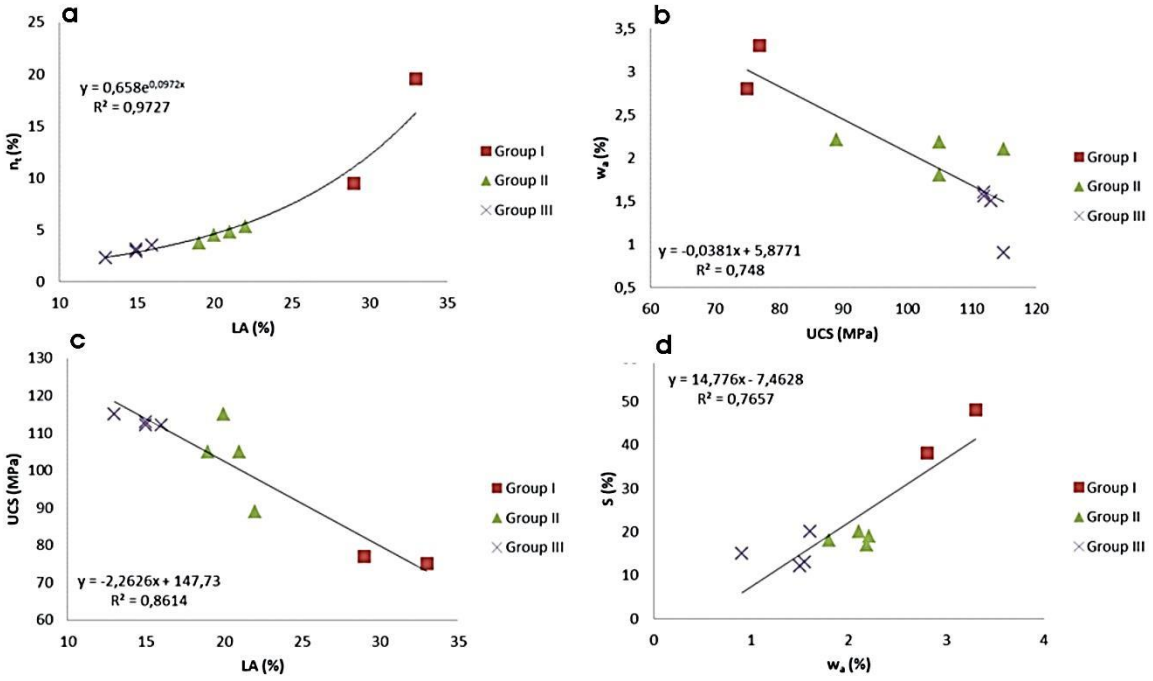

Figure 6. (**a**) Los Angeles abrasion value (LA) of the studied rock samples plotted against total porosity (nt); (**b**) Uniaxial compressive strength (UCS) of the studied rock samples plotted against water absorption (W_a); (**c**) Los Angeles abrasion value (LA) of the studied rock samples plotted against their uniaxial compressive strength (UCS); (**d**) Water absorption (W_a) of the studied rock samples plotted against the soundness test (S).

In contrast to the comparatively finer grained sandstones, molecular internal forces are developed during the loading presenting better cohesion and bonding among the grains. Furthermore, the porosity (n_t) as well as the water absorption (w_a) seems to significantly be increased in the coarse sandstone rocks against the fine ones, which indicates that larger grains exhibiting weaker cohesion in contrast to the smaller are capable to adsorb more percentage of water

Peer-reviewed version available at Energies 2020, 13, 1119; doi:10.3390/en13051119

around each grain mainly in the form of a surface layer. The diagram in Figure 6c illustrates the interaction of the mechanical properties LA and UCS directly dependent on the grain size. Several researchers have also reported similar relationships between these properties [23, 65, 69, 70] when studying various types of rocks. In this diagram, it seems obvious that the mechanical characteristics of sandstones vary in a similar way under different type of mechanical loadings. For example, rocks of Group I (coarse grained) present lower resistance in abrasion and attrition and lower compressive strength in contrast to those of Group III (fine grained) which presented as more resistant in abrasion and attrition and with higher strength values. In the diagram of figure 6d, the relationship between the Soundness test (S) and the water absorption (w_a) is presented, the trend of which is similar to other reported relationships between the Soundness test and physical properties by several researchers [61]. The interpretation given above regarding the ability of coarse grained sandstones to adsorb water in their structure in contrast to the fine grained sandstones has a strong effect on their resistance to temperature changes. All of the above theories regarding the effect of grain size on the physico-mechanical properties of rocks are quantified and presented below in Figure 7. More specifically, the quantification of the number of minerals per mm² (C/A) (calculated via GIS) seems to be strongly correlated with the physico-mechanical properties of the sandstones. In Figure 7a, it can be seen that as the C/A increases, the strength of the rocks increases (Figure 7a) and their resistance in abrasion and attrition increases respectively (Figure 7b), whereas the number of minerals per mm² increases as their porosity decreases (Figure 7c). It is noticeable that the above mentioned relationships display high coefficient of correlation (R^2=0.72 and R^2=0.71) (Table 4) a fact that enhances that the grain size constitutes the principal but not the unique factor which influences these properties. This happens because the mineralogical composition of rocks also determines their physicomechanical properties.

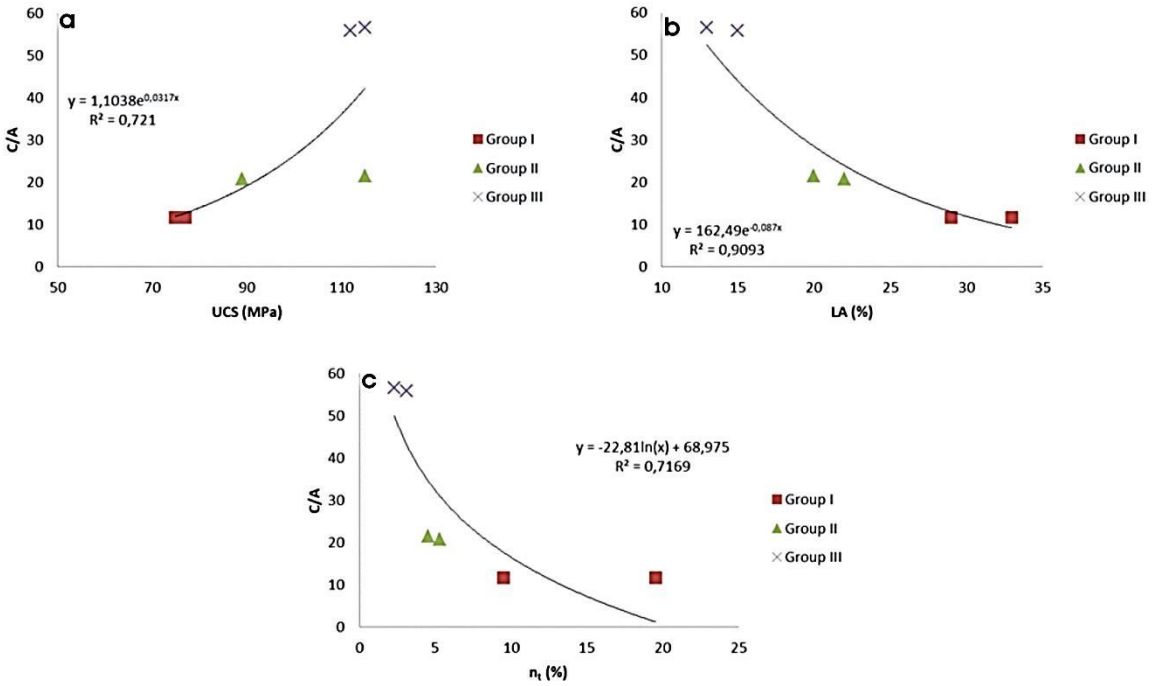

Figure 7. (**a**) Uniaxial compressive strength (UCS) of the studied rock samples plotted against the ratio C/A; (**b**) Los Angeles abrasion (LA) of the studied rock samples plotted against the ratio C/A; (**c**) Total porosity (n_t) of the studied rock samples plotted against the ratio C/A.

Concerning the produced from the investigated sandstone concretes; they present satisfactory values of compressive strength (24.00 to 32.00 MPa) relative to other concrete specimens which have been made by andesites and serpentinites as aggregate particles [22]. These satisfactory strength results may attributed to the generally high microtopography of coarse grained, medium grained as well as of fine grained sandstones relative to the microtopography of other used rocks [22] (Figure 2b, d, f, h, figure 4). The microtopography of the aggregates constitutes a crucial factor for the

Peer-reviewed version available at Energies 2020, 13, 1119; doi:10.3390/en13051119

mechanical quality of the aggregate rocks and consequently for the quality of the produced concrete as it influences the cohesion and the bonding between the cement paste and the aggregate particles [1, 22, 23]. The only studied concrete specimen which displays lower strength (25 MPa) than the standard states is the specimen in which the used aggregate was the enriched in carbonate fossils coarse grained sandstone (Figure 2 c). This fact may be the result of the lower resistance of the fossils which tend to be broken during the mechanical loading, combined with the low microtopography which they promote (Figure 3d). However, although all the investigated concrete specimens revealed satisfactory strength results, small differences in their values appeared depending on the grain size of the sandstones. The total of the diagrams of Figure 8 indicate that the aggregate properties, which are determined by the size and the number of the grains, as it is shown in Figure 7, determine the final strength of the produced concrete specimens.

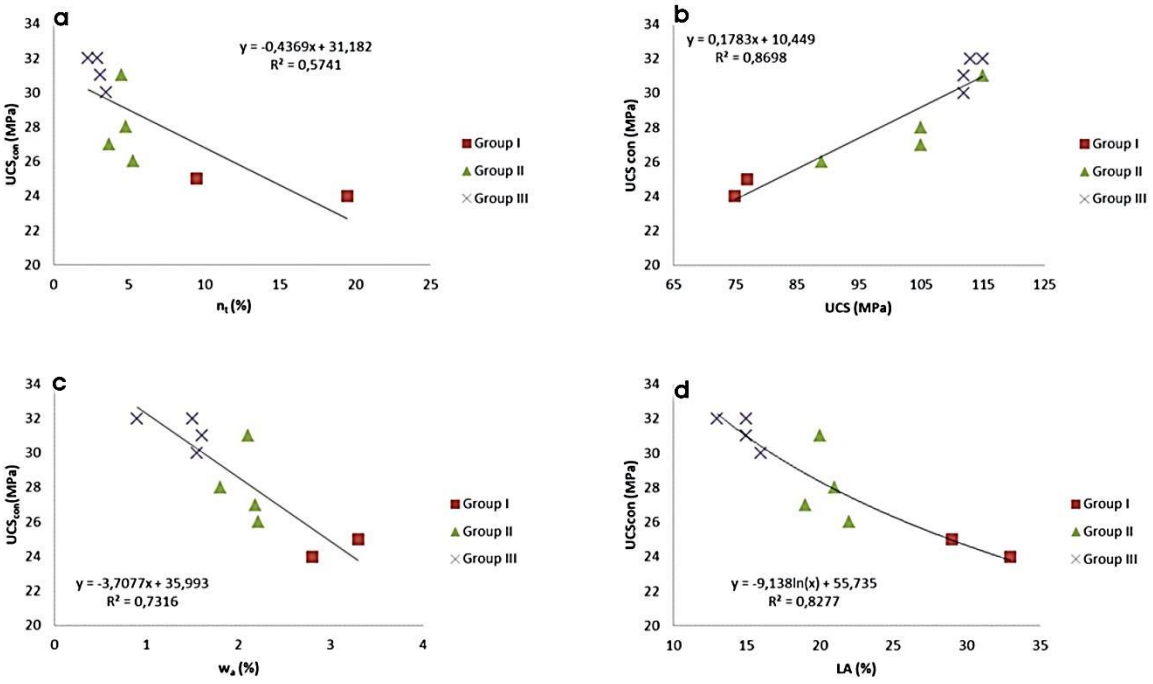

Figure 8. (**a**) Total porosity (n_t) of the studied rock samples plotted against the uniaxial compressive strength of concrete (UCS_{con}); (**b**) Uniaxial compressive strength of the tested rock samples plotted against the uniaxial compressive strength of concrete (UCS_{con}); (**c**) Water absorption (w_a) of the studied rock samples plotted against the uniaxial compressive strength of concrete (UCS_{con}); (**d**) Los Angeles abrasion value (LA) of the studied rock samples plotted against the uniaxial compressive strength of concrete (UCS_{con}).

During the petrographic analysis of the tested concrete specimens, no significant failures and loss of material were observed in those produced by coarse grained sandstones and nor extensive reaction zones, which typically occur in igneous high porosity aggregates. One possible interpretation that can be attributed is that the lower mechanical strength of concrete aggregates may depend on the higher porosity of the coarse grained sandstones in contrast to the fine grained ones (Table 2) which result in the greater adsorption of water which is useful during the 28 days of curing for the achievement of the optimum cohesion between the cement paste and the aggregate particles. However, such extensive areas of incomplete hydration of the cement around the grains were not observed during petrographic examination of the concrete using polarizing microscope. This may have happened due to the evenly distribution of the mineralogical composites of rocks as can be seen in the 3D depiction via GIS. This resulted in the evenly adsorption of water and consequently these zones cannot be easily perceived.

Table 4. Correlation equations of diagrams of Figure 6, Figure 7 and Figure 8

Correlation equations of diagrams of Figure 6, Figure 7 and Figure 8

Peer-reviewed version available at Energies 2020, 13, 1119; doi:10.3390/en13051119

Diagram	R^2	Equation
6a	0.97	$n_t=0.658e^{0.0972LA}$
6b	0.74	$w_a=-0.0381UCS+5.8771$
6c	0.86	$UCS=-2.2626LA+147.73$
6d	0.76	$S=14.776w_a-7.4628$
7a	0.72	$C/A=1.1038e^{0.0317UCS}$
7b	0.90	$C/A=162.49e^{-0.087LA}$
7c	0.71	$C/A=-22.81\ln(n_t)+68.975$
8a	0.57	$UCS_{con}=-0.4369n_t+31.182$
8b	0.86	$UCScon=0.1783UCS+10.449$
8c	0.73	$UCS_{con}=-3.7077w_a+35.993$
8d	0.82	$UCS_{con}=-9.138\ln(LA)+55.735$

5.2. A potential scenario for storage of CO_2 in sandstones from Klepa Nafpaktias

The studied area presents an appropriate geological basin environment for applying CO_2 capture and storage (CCS) applications. It is well known that the permeability of flysch formations is regarded as being generally low due to the presence of marl and clay intercalations within this type of formation. This practically impermeable sedimentary formation lies stratigraphically above the sandstones, thus providing an excellent seal caprock to keep the buoyant CO_2 within the reservoir rock. This case presents many similarities with that described for the Mesohellenic Trough (NW Greece), which examined the potential of CO_2 storage within porous sandstones that are overlaid be a less permeable cap rock formation [71-73]. In the latter case, a depth of over 800m was regarded as suitable for trapping CO_2 under supercritical conditions [73-75]. The sandstone samples provided from our study are highly comparable in terms of composition with sandstones from the Pentalofos formation of the Mesohellenic Trough [72]. Petrographic and mineral modal examinations reveal that the sandstones (Group I, II, III) from Klepa Nafpaktias display the following modal compositions: Quartz=24-29%; K-feldspar=7-29%; Calcite=1-8%; Muscovite=1-4%; Plagioclase~0.5%; Siliceous and Calcite-bearing Cement=42-57% (Figure 2, Table 1).

These results show that the sandstones examined include relatively higher quartz contents and less calcite compared to those located in the Mesohellenic Trough [73]. Furthermore, effective porosity of the Klepa Nafpaktias sandstones, as it was calculated through the total porosity, which is about 6% for the Group I presents higher values of effective porosity in contrast to the other two sandstone groups and tend to be lower than the Pentalofos sandstones of the Mesohellenic Trough ~ 9%.

Despite the relatively smaller storage potential presented in the region of Klepa Nafpaktias, the rather higher silica contents offers the ability of avoiding undesirable fracture development and disintegration phenomena. This is because CO_2 is expected to react with calcite hosted within the sandstones; however, this would result in the formation of unstable bicarbonates, which would hinder their ability for permanent CO_2 storage. Recent studies on CO_2 geological storage within sandstone formations reveal the importance of feldspar and plagioclase minerals for permanent CO_2 trapping [e.g.75-78].

The mineralogical composition of the studied sandstones of Group I as well as their general petrographic characteristics enhances their capacity for CO_2 storage as the sufficient amounts of K-feldspars can react with injected supercritical CO_2 with the following reactions (1-4):

$$\mathbf{2KAlSi_3O_8\,(K\text{-}feldspar) + CO_2 + 2H_2O \Rightarrow Al_2(Si_2O_5)(OH)_4(kaolinite) + 4SiO_2 + K_2CO_3} \quad \mathbf{(1)}$$

$$\mathbf{3KAlSi_3O_8\,(K\text{-}feldspar) + H_2O + CO_2 \Rightarrow KAl_3Si_3O_{10}(OH)_2(illite) + 6SiO_2 + K_2CO_3} \quad \mathbf{(2)}$$

$$\mathbf{2NaAlSi_3O_8\,(albite) + 2CO_2 + 3H_2O \Rightarrow Al_2(Si_2O_5)(OH)_4(kaolinite) + 4SiO_2 + 2Na^{+} + 2HCO^{-3}} \quad \mathbf{(3)}$$

Peer-reviewed version available at Energies 2020, 13, 1119; doi:10.3390/en13051119

$NaAlSi_3O_8$ (albite) + CO_2+H_2O⇒$NaAlCO_3(OH)_2$(dawsonite)+3SiO_2 (4)

Thus, the dissolution of alkali feldspars will lead to the precipitation of clay minerals and silica (in the form of quartz). Plagioclase, although present in smaller amounts, is also expected to produce kaolinite, as well as calcite through the successive reactions (5) and (6):

$CaAl_2Si_2O_8$ (anorthite)+2CO_2+3H_2O ⇒ $Al_2(Si_2O_5)(OH)_4$(kaolinite)+Ca^{2+}+2HCO^{-3} (5)

$CaAl_2Si_2O_8$ (anorthite) + H_2CO_3+ H_2O ⇒ $Al_2Si_4O_5(OH)_4$(kaolinite) + $CaCO_3$ (6)

We provide preliminary calculations that estimate the CO_2 that could be stored in the frames of a potential pilot project in the studied region. For this purpose, we apply the function below:

$$\text{Storage Capacity} = \sum(V \times \phi \times \varrho \times \varepsilon)$$

where V is the volume of the sandstone reservoir (under the flysch cap rock); ϕ is the average effective porosity; ϱ is the specific gravity of the sCO_2; and ε is the sCO_2 storage ratio. A potential pilot project can be realized at an estimated volume of 5000 m (length) × 3000 m (width) × 500 m (depth) = 75 × 10^8. Based upon the estimations of Jin et al. [75] and with reference to the statistical values of USGS modeling, we can consider the CO_2 storage ratio for sandstones to be 1%. The application of this discount factor is necessary in order to obtain a realistic estimation of the sandstone reservoir storage potential. Taking the aforementioned value into consideration, as well as the average effective porosity of sandstones from our studied site (6%) and the specific gravity of the supercritical CO_2 (400 kg/m^3; at 10 MPa and 50◦C [79], the demarcated area could potentially store an amount of 18 × 10^5 tons of CO_2.

We also consider equation (12) of Jin et al. [75] to calculate the quantity of CO_2 trapped by feldspars (K-feldspar and plagioclase minerals, where these amounts K-feldspar=23-34%; Plagioclase=~1% resulted from the reduction of the initial amounts without the cement):

$$m\text{CO2 Feldspar} = [p\text{Feldspar} \times V \times (1 - \varphi) \times X\text{Feldspar} \times M\text{CO2} \times R] / M\text{Feldspar}$$

where V is the volume of the sandstone reservoir, ϕ is the average effective porosity, $p_{Feldspar}$ is the feldspar density (2.55–2.67 × 10^3, 2.55–2.60 × 10^3 and 2.75–2.76 × 10^3 kg/m^3 for K-feldspar, albite and anorthite respectively), $M_{Feldspar}$ is molecular weight (279.07, 262.96 and 278.94 for K-feldspar, albite and anorthite respectively) R is the ratio of feldspar mineral to CO_2 0.5, 1 and 1 for K-feldspar, albite and anorthite respectively), $X_{Feldspar}$ the proportions of feldspar minerals, M_{CO2} is the total CO_2 storage capacity of mineral trapping. By applying this equation upon alkali feldspars and plagioclase the results calculated for the CO_2 that can be permanently trapped within the sandstone formation is ~6 × 10^5 tons, which is less by almost approximately 1/3 of the storage potential calculated with the previous method. This is due to the fact that the latter equation does not consider calcite crystallization as a stable mineral phase. Nevertheless, considering both cases, it is evident that the sandstones of the Klepa Nafpaktias region are capable of storing sufficient amounts of CO_2. This is even more evident taking into consideration that region's sandstones and flysch formations encompasses an even wider area and thus could allow for the deployment of larger-scale CO_2 storage projects, provided that the proposed pilot test is deployed successfully.

6. Conclusions

In this paper, sandstones of various petrographic characteristics derived from Klepa Nafpaktias were examined in order to evaluate their suitability in construction (concrete) and environmental applications (CO_2 storage). For the first time, the petrographic study of rocks such as of those sandstones were carried out by using classic petrographic methods (observation through polarizing microscope) combined with modern tools of quantification of modal composition (GIS proposed

Peer-reviewed version available at Energies 2020, 13, 1119; doi:10.3390/en13051119

method) and 3D depictions of their petrographic features (3D Builder software). The above mentioned study leads to the following concluding remarks:

- Three groups of sandstones were detected according to their petrographic features regarding the grain size (coarse, medium and fine grained size).
- The above classification of rocks was retained in their physicomechanical and physicochemical properties as well as in the final strength of the produced concrete specimens.
- The petrographic observation of thin sections of the concrete specimens combined with the results of their mechanical strength revealed that the studied sandstones are suitable for concrete aggregates (Group I, II, III) except one coarse grained sample (K.L9 (Group I)) which contains intense amount of carbonate fossils presenting lower concrete strength than the standard states.
- The proposed ratio C/A (crystals/ mm^2) seems to influence the aggregate properties which constitute critical factors for the final concrete strength, presenting the more fine grained sandstones as the most suitable for concrete aggregates.
- The petrographic characteristics of the sandstones from Klepa Nafpaktias and their porosity values reveal that the coarse grained samples (Group I) is more capable for potential CO_2 storage.
- Preliminary calculations suggest that a potential pilot project can store an amount of up to 18×10^5 tons CO_2. The size of the sandstones formation provides the necessary basis for examining the deployment of an even larger scale pilot test that suggested from the present study.

Author Contributions: P.P. participated in the fieldwork, the elaboration of laboratory tests, the interpretation of the results, coordinated the research and wrote the manuscript; P.P.G. participated in the fieldwork, the elaboration of laboratory tests, the interpretation of the results and contributed to the manuscript writing; A.R. participated in the fieldwork, the interpretation of the results and contributed to the manuscript writing; M.K. participated in the fieldwork, modified the geological map and performed the GIS analysis; P.K. participated in the interpretation of the results and contributed to the manuscript writing; M.E.D. participated in the fieldwork and in the elaboration of laboratory tests and N.K. participated in the interpretation of the results and contributed to the manuscript writing.

Funding: This research received no external funding.

Acknowledgments: The authors wish to thank Dr. A.K Seferlis of the Laboratory of Electron Microscopy and Microanalysis, University of Patras for his assistance with the microanalyses and SEM micrographs.

Conflicts of Interest: The authors declare no conflict of interest.

References

1. Petrounias, P.; Giannakopoulou, P.P.; Rogkala, A.; Lampropoulou, P.; Tsikouras, B.; Rigopoulos, I.; Hatzipanagiotou, K. Petrographic and Mechanical Characteristics of Concrete Produced by Different Type of Recycled Materials. *Geosciences* **2019**, *9*, 264.
2. Farzadnia, N.; Abang, A.A.A.; Demirboga, R.; Anwar, M.P. Effect of halloysite nanoclay on mechanical properties, thermal behavior and microstructure of cement mortars. *Cem. Concr. Res.* **2013**, *48*, 97-104.
3. Tamanna, N.; Sutan, N.M.; Lee, D.T.C. Utilization of waste glass in concrete. 6th International Engineering Conference, Energy and Environment (ENCON), 2013, Published by Research Publishing.
4. Castro, S.; Brito, J. Evaluation of the durability of concrete made with crushed glass aggregates. *J. Clean. Prod.* **2013**, *41*, 7-14.
5. Abdallah, S.; Fan. M. Characteristics of concrete with waste glass as fine aggregate replacement. *J. Eng. Technol. Res.* **2014**, *2*, 11-17.
6. Jani, W.; Hogland, W. Waste glass in the production of cement and concrete – A review. *J. Envir. Chem. Eng.* **2014**, *2*, 1767-1775.
7. Meng, Y.; Ling, T.G.; Mo, K.H. Recycling of wastes for value-added applications in concrete blocks: An overview. *Resour. Conserv. Recycl.* **2018**, *138*, 298-312.

8. Poon, C.S.; Chan, D. Paving blocks made with recycled concrete aggregate and crushed clay brick. *Constr. Build. Mater.* **2006**, *20 (8)*, 569-577.
9. Vanitha, S.; Natrajan, V.; Prada, M. Utilization of waste plastics as a partial replacement of coarse aggregate in concrete blocks. *Indian J. Sci. Technol.* **2015**, *8 (12)*, 256-268.
10. Jackson, N. Civil Engineering Materials; Macmillan Press Ltd.: London, UK, 1981.
11. LaLonde, W.S.; Janes, M.F. Concrete Engineering Handbook; Library of Congress: New York, NY, USA, 1961.
12. US Concrete Industry Report; Library of Congress: New York, NY, USA, 2001.
13. Neville, A.M. Properties of Concrete, ELSB 5th ed.; Pearson Education Publishing Ltd.: London, UK, 2005.
14. Taylor, G.D. Materials in Construction, 2nd ed.; Longman Group Ltd., Longman House, Burnt Mill: Harlow, UK, 1994.
15. Neville, A.M. Properties of Concrete, 4th ed.; Pitman: London, UK, 1995.
16. Al-Oraimi, S.K.; Taha, R.; Hassan, H.F. The effect of the mineralogy of coarse aggregate on the mechanical properties of high-strength concrete. *Constr. Build. Mater.* **2006**, *20*, 499–503.
17. Mackechnie J.R. Shrinkage of concrete containing greywake sandstone aggregate. *Aci Materials Journal* **2006**, *103 (5)*, 390-396.
18. Rodgers, M.; Hayes, G.; Healy, M.G. Cyclic loading tests on sandstone and limestone shale aggregates used in unbound forest roads. *Constr. Build. Mater.* **2009**, *23*, 2421-2427.
19. Verstrynge, E.; Schueremans, L.; Van Gement, D. Creep and failure prediction of diestian ferruginous sandstone: modelling and repair options, Constr. Build. Mater. 29 (2012) 149-157.
20. Kumar, S.; Gupta, R.C.; Shrivastava, S. Strength, abrasion and permeability studies on cement concrete containing sandstone coarse aggregates. *Constr. Build. Materials* **2016**, *125*, 884-891.
21. Yilmaz, M.; Tugrul, A. The effects of different sandstone aggregates on concrete strength. *Constr. Build. Mater.* **2012**, *35*, 294–303. doi:10.1016/j.conbuildmat.2012.04.014.
22. Petrounias, P.; Giannakopoulou, P.P.; Rogkala, A.; Stamatis, P.M.; Tsikouras, B.; Papoulis, D.; Lampropoulou, P.; Hatzipanagiotou, K. The Influence of Alteration of Aggregates on the Quality of the Concrete: A Case Study from Serpentinites and Andesites from Central Macedonia (North Greece). *Geosciences* **2018a**, *8*, 115.
23. Petrounias, P.; Giannakopoulou, P.P.; Rogkala, A.; Stamatis, P.M.; Lampropoulou, P.; Tsikouras, B.; Hatzipanagiotou, K. The Effect of Petrographic Characteristics and Physico-Mechanical Properties of Aggregates on the Quality of Concrete. *Minerals* **2018c**, *8*, 577.
24. Li, Y.; Onasch, M.C.; Guo, Y. GIS-based detection of grain boundaries. *J. Struct. Geol.* **2008**, *30*, 431–443.
25. Barraud, J. The use of watershed segmentation and GIS software for textural analysis of thin sections. *J. Volcanol. Geotherm. Res.* **2006**, *154*, 17–33.
26. Fernandez, F.J.; Menendez-Duarte, R.; Aller, J.; Bastida, F. Application of geographical information systems to shape-fabric analysis. In: High-Strain Zones: Structure and Physical Properties, 245. Edited by D. Bruhn and L. Burlini, Geological Society of London Special Publication, 409–420, 2005.
27. Tarquini, S.; Favalli, M. A Microscopic Information System (MIS) to assist in petrographic analysis. *Comput. Geosci.* **2010**, *36*, 665-674.
28. Becattini, V.; Motmans, T.; Zappone, A.; Madonna, C.; Haselbacher, A.; Steinfeld, A. Experimental investigation of the thermal and mechanical stability of rocks for high-temperature thermal-energy storage. *Appl. Energy* **2017**, *203*, 373-389.
29. Kuravi, S.; Trahan, J.; Goswami, D.Y.; Rahman, M.M.; Stefanakos, E.K. Thermal energy storage technologies and systems for concentrating solar power plants. *Prog. Energy Combust. Sci.* **2013**, *39*, 285–319.
30. Khare, S.; Dell' Amico, M.; Knight, C.; Mc Garry, S. Selection of materials for hightemperature sensible energy storage. *Solar Energy Mater. Solar Cells* **2013**, *115*, 114–22.
31. Allen, K.G.; von Backström, T.W.; Kröger D.G.; Kisters, A.F.M. Rock bed storage for solar thermal power plants: rock characteristics, suitability, and availability. *Solar Energy Mater. Solar Cells* **2014**, *126*, 170–83.
32. Tiskatine, R.; Eddemani, A.; Gourdo, L.; Abnay, B.; Ihlal, A.; Aharoune, A.; et al. Experimental evaluation of thermo-mechanical performances of candidate rocks for use in high temperature thermal storage. *Appl. Energy* **2016**, *171*, 243–55.

33. Karakitsios, V., Tzortzaki, E.; Giraud, F.; Pasadakis, N. First evidence for the early Aptian Oceanic Anoxic Event (OAE1a) from the Western margin of the Pindos Ocean (NW Greece). *Geobios.* **2018**, *51*, 187-210.
34. Robertson, A.H.F.; Karamata, S. The role of subduction-accretion processes in the tectonic evolution of the Mesozoic Tethys in Serbia. *Tectonophysics* **1994**, *234*, 73–94.
35. Aubouin, J.; Bonneau, M.; Davidson, G.J.; Leboulenger, P.; Matesko, S.; Zambetakis, A. Esquisse structurale de l'Arc egeen externe : des Dinarides aux Taurides. *Bull. Soc. Géol. Fr.* **1976**, *7 (18)*, 327–336.
36. Bernoulli, D.; De Graciansky, P.C.D.; Monod, O. The extension of the Lycian Nappes (SW Turkey) into the Southeastern Aegean Islands. *Eclogae Geol. Helv.* **1974**, *67*, 39–90.
37. Argyriadis, I.; De Graciansky, P.C.; Marcoux, J.; Ricou, L.E. The opening of the Mesozoic Tethys between Eurasia and Arabia-Africa. In: Aubouin, J., Debelmas, J., Latreille, M. (Eds.), Geologie des chaınes alpines issues de la Tethys, 26th International Geological Congress, Paris, Colloque C5. *Bureau de Recherches Geologiques et Minieres Memoire* **1980**, *115*, 199–214.
38. Kafousia, N.; Karakitsios, V.; Jenkyns, H.C.; Mattiolis, E. A global event with a regional character: the Early Toarcian Oceanic Anoxic Event in the Pindos Ocean (northern Peloponnese, Greece). *Geol. Mag.* **2011**, *148 (4)*, 619–631.
39. Fleury, J.J. Les zones de Gavrovo-Tripolitza et du Pinde-Olonos (Grece continentale et Peloponese du nord) Evolution d'une plate-forme et d'un basin dans leur cadre alpin. *Societe Geologique du Nord* **1980**, *4*, 1–473.
40. De Wever, P.; Baudin, F. Palaeogeography of radiolarite and organic-rich deposits in Mesozoic Tethys. *Geologische Rundschau* **1996**, *85*, 310–26.
41. Clift, P.D. The collision tectonics of the southern Greek Neotethys. *Geologische Rundschau* **1992**, *81*, 669–79.
42. Degnan, P.J.; Robertson, A.H.F. Mesozoic–early Tertiary passive margin evolution of the Pindos Ocean (NW Peloponnese Greece). *Sediment. Geol.* **1998**, *117*, 33–70.
43. Pe-Piper, G. The nature of Triassic extension-related magmatism in Greece: evidence from Nd and Pb isotope geochemistry. *Geol. Mag.* **1998**, *135*, 331–48.
44. Neumann, P.; Zacher, W. The Cretaceous sedimentary history of the Pindos Basin Greece. *Int. J. Earth Sci.* **2004**, *93*, 119–131.
45. Konstantopoulos, P.A.; Zelilidis, A. Sedimentation of submarine fan deposits in the Pindos foreland basin, from late Eocene to early Oligocene, west Peloponnesus peninsula, SW Greece. *Geol. J.* **2013**, *48*, 335–362.
46. Jones, G.; Robertson, A.H.F.; Cann, J.R. Genesis and emplacement of the suprasubduction zone Pindos Ophiolite, northwestern Greece. In: Peters T., Nicolas A. & Coleman S. (Eds.): Ophiolite genesis and evolution of the oceanic lithosphere. *Sultanate of Oman Ministry of Petroleum and Minerals* **1991**, 771—799.
47. Faupl, P.; Pavlopoulos, A.; Migiros, G. On the provenance of flysch deposits in the External Hellenides of mainland Greece: results from heavy mineral studies. *Geol. Mag*. **1999**, *135 (3)*, 412–442.
48. Vakalas, I. Evolution of Foreland Basins in Western Greece. PhD dissertation, University of Patras, Greece, 373, 2004.
49. Loftus, D.L.; Matarangas, D.; Zindros, G.; Katsikatsos, G. Geological Map of Greece, Klepa Sheet, 1:50.000; IGME: Athens, Greece, 1984.
50. Part 1: Composition, Specifications and Conformity Criteria for Common Cements; EN 197-1; European Standard: Warsaw, Poland, 2011.
51. Part 3: Procedure and Terminology for Simplified Petrographic Description; EN 932; European Standard: Warsaw, Poland, 1996.
52. Methods for Sampling and Testing of Mineral Aggregates, Sands and Fillers, Part 1: Methods for Determination of Particle Size and Shape; BS 812; British Standard Institution: London, UK, 1975.
53. ISRM Suggested Methods. Rock Characterization Testing and Monitoring; Brown, E., Ed.; Pergamon Press: Oxford, UK, 1981.
54. EN 1367-2. Tests for Thermal and Weathering Properties of Aggregates—Part 2: Magnesium Sulfate Test; European Committee for Standardization: Brussels, Belgium, 1999.
55. EN 1097-6, Tests for mechanical and physical properties of aggregates – Part 6: Determination of particle density and water absorption. European Committee for Standardization: Brussels; 2000.

56. ASTM C-131. Resistance to Abrasion of Small-Size Coarse Aggregate by Use of the Los Angeles Machine; American Society for Testing and Materials: Philadelphia, PA, USA, 1989.
57. Standard Test Method for Unconfined Compressive Strength of Intact Rock Core Specimens; ASTM D 2938-95; American Society for Testing and Materials: West Conshohocken, PA, USA, 2002.
58. Standard for Selecting Proportions for Normal, Heavyweight and Mass Concrete; ACI-211.1-91; American Concrete Institute: Farmington Hills, MI, USA, 2002.
59. Part 3: Testing Hardened Concrete. Compressive Strength of Test Specimens; BS EN 12390; British Standard Institution London, UK, 2009.
60. Standard Practice for Petrographic Examination of Hardened Concrete; ASTM C856; American Society for Testing and Materials: West Conshohocken, PA, USA, 2017.
61. Rigopoulos, I.; Tsikouras, B.; Pomonis, P.; Hatzipanagiotou, K. The impact of petrographic characteristics on the engineering properties of ultrabasic rocks from northern and central Greece. *Q. J. Eng. Geol. Hydrogeol*. **2012**, *45*, 423–433. doi:10.1144/qjegh2012-021.
62. Smith, M.R.; Collis, L. Aggregates: Sand, Gravel and Crushed Rock Aggregates for Construction Purposes; Spec. Publ. 17; The Geological Society: London, UK, 2001.
63. Hartley, A. A review of the geological factors influencing the mechanical properties of road surface aggregates. *Q. J. Eng. Geol.* **1974**, *7*, 69–100.
64. Barttli, B. The influence of geological factors on the mechanical properties of basic igneous rocks used as road surface aggregates. *Eng. Geol*. **1992**, 33, 31–44.
65. Petrounias, P.; Giannakopoulou, P.P.; Rogkala, A.; Lampropoulou, P.; Koutsopoulou, E.; Papoulis, D.; Tsikouras, B.; Hatzipanagiotou, K. The Impact of Secondary Phyllosilicate Minerals on the Engineering Properties of Various Igneous Aggregates from Greece. *Minerals* **2018b**, 8, 329. doi:10.3390/min8080329.
66. Turgul, A.; Zarif, I.H. Correlation of mineralogical and textural characteristics with engineering properties of selected granitic rocks from Turkey. *Eng. Geol*. **1999**, 51, 303–317.
67. Rigopoulos, I.; Tsikouras, B.; Pomonis, P.; Hatzipanagiotou, K. Correlations between petrographic and geometrical properties of ophiolitic aggregates from Greece. *Bull. Eng. Geol. Environ.* **2014, 73, 1-12**.
68. Escartin, J.; Hirth, G.; Evans, B. Strength of slightly serpentinized peridotites: Implications for the tectonics of oceanic lithosphere. *Geology* **2001**, 29, 1023–1026.
69. Giannakopoulou, P.P.; Petrounias, P.; Rogkala, A.; Tsikouras, B.; Stamatis, P.M.; Pomonis, P.; Hatzipanagiotou, K. The influence of the mineralogical composition of ultramafic rocks on their engineering performance: A case study from the Veria-Naousa and Gerania ophiolite complexes (Greece). Geosciences 2018, 8, 251. doi:10.3390/geosciences8070251.
70. Giannakopoulou, P.P.; Petrounias, P.; Tsikouras, B.; Kalaitzidis, S.; Rogkala, A.; Hatzipanagiotou, K.; Tombros, S.F. Using Factor Analysis to Determine the Interrelationships between the Engineering Properties of Aggregates from Igneous Rocks in Greece. *Minerals* **2018**, *8*, 580.
71. Koukouzas, N.; Ziogou, F.; Gemeni, V. Preliminary assessment of CO_2 geological storage opportunities in Greece. *Int. J. Greenh. Gas Con.* **2009**, *3*, 502-513.
72. Tassianas, A.; Koukouzas, N. CO_2 Storage Capacity Estimate in the Lithology of the Mesohellenic Trough, Greece. *Energy Procedia* **2016**, *86*, 334-341.
73. Koukouzas, N.; Kypritidou, Z.; Purser, G.; Rochelle, C.A.; Vasilatos, C.; Tsoukalas, N. Assessment of the impact of CO_2 storage in sandstone formations by experimental studies and geochemical modeling: The case of the Mesohellenic Trough, NW Greece. *Int. J. Greenh. Gas Con.* **2018**, *71*, 116-132.
74. Shafeen, A.; Croiset, E.; Douglas, P.L.; Chatzis, I. CO_2 sequestration in Ontario, Canada. Part I: storage evaluation of potential reservoirs. *Energy Convers. Manage.* **2004**, *45*, 2645–2659.
75. Jin, C.; Liu, L.; Li, Y.; Zeng, R. Capacity assessment of CO_2 storage in deep saline aquifers by mineral trapping and the implications for Songliao Basin, Northeast China. *Energy Sci. Eng.* **2017**, *5 (2)*, 81–89.
76. Ryoji, S.; Thomas, L.D. Experiment al study on water-rock interactions during CO_2 flooding in the Tensleep Formation, Wyoming, USA. *Appl. Geochem* **2000**, *15*, 265–279.
77. Robert, J.R.; Tamer, K.; James, L.P. Experiment al investigation of CO_2- brine-rock interactions at elevated temperature and pressure: implications for CO_2 sequestration in deep-saline aquifers. *Fuel Process. Technol.* **2005**, *86*, 1581–1597.
78. Ryzhenko, B.N. Genesis of dawsonite mineralization: thermo-dynamic analysis and alt ernative. *Geochem. Int.* **2006**, *44*, 835–840.

Peer-reviewed version available at *Energies* **2020**, *13*, 1119; doi:10.3390/en13051119

79. Spycher, N.; Pruess, K. CO_2-H_2O Mixtures in the Geological Sequestration of CO_2. II. Partitioning in Chloride Brines at 12-100°C and up to 600 bar. *Geochim. Cosmochim. Acta* **2005**, *69 (13)*, 3309-3320.